JMEPEG (2005) 14:574-581
DOI: 10.1361/105994905X64512

1059-9495/$19.00

# Mathematical Model for Austenitization Kinetics of Ductile Iron

*Uma Batra, S. Ray, and S.R. Prabhakar*

*(Submitted February 16, 2005; in revised form June 27, 2005)*

**A mathematical model was developed in the current study to understand the progress of austenitization process in ductile irons. The austenitization time required to produce homogeneous austenite in a two-phase region of austenite and graphite has been estimated in terms of (a) time required for transformation of matrix to austenite and (b) time required for dissolution of graphite in austenite to attain uniform carbon content, which remains in equilibrium with graphite. The time required been related to the structural parameters of cast ductile iron-like radius of graphite nodule, radius of austenite cell, volume fraction of graphite, volume fraction of ferrite in cast matrix, and diffusion constant. The model was used to determine the minimum austenitization time required to achieve homogeneous austenite in three commercial ductile irons when austenitized at a temperature of 900 °C. The results were compared with those obtained. The uniformity of the carbon content in austenite of ductile iron was verified indirectly by measuring microhardness.**

**Keywords** austenitization, diffusion, ductile iron, kinetics, mathematical model, x-ray diffraction,

## 1. Introduction

Ductile iron has graphite nodules embedded in a matrix of ferrite or ferrite and pearlite. A wide range of microstructure and properties of the ductile iron could be obtained through heat treatments by the phase transformation of its as-cast matrix (Ref 1, 2). For example, development of Austempered Ductile Iron by heat treatment has gained wide spread popularity (Ref 3-5). Austenitization of the matrix is a prerequisite of any such phase transformation, and the analysis of the process taking place during the heat treatment is essential for precise control of structure and properties in heat-treated ductile iron (Ref 6).

In the present investigation, the austenitization process for ductile irons has been analyzed through mathematical model in order to estimate the optimum time required to obtain homogeneous austenite with carbon content, which remains in equilibrium with the graphite nodules. The austenitization time has been related to the variables like austenitization temperature, initial carbon content of matrix, size of graphite nodules, and the nodule count, which determines the size of matrix cell surrounding the nodule. Proper selection of austenitization time will help the heat-treater to avoid (a) incomplete or inhomogeneous austenitization due to lack of austenitization time and (b) excessive grain growth due to longer austenitization time.

**Uma Batra,** Punjab Engineering College, Department of Metallurgical Engineering, Chandigarh, 160012 India; **S. Ray,** Department of Metallurgical and Materials Engineering, 11T Roorkee, India; and **S.R. Prabhakar,** Principal Indo Global College of Engineering and Technology, India. Contact e-mail: umabatra2@yahoo.com.

## 2. Inputs of Model

The symbols and units for various variables used throughout the paper are defined in Table 1. The ductile iron is considered to consist of a large number of spherical cells of equal size. Each cell has a graphite nodule at its center, surrounded by the matrix structure. It is assumed that all the graphite nodules are of equal size. The matrix structure surrounding the graphite nodule in the cell may be ferrite, pearlite, or ferrite + pearlite. Figure 1 gives a schematic representation of the different forms of ductile irons. In case of ductile iron with ferrite + pearlite matrix, a thin ferrite region surrounds the graphite nodule, and the rest of the cell consists of ferrite as well as pearlite. The ratio of ferrite to pearlite areas depends upon the initial carbon content of the matrix. The primary model inputs will be the radius of graphite nodule $r_g$, radius of each cell $r_{cell}$, volume fraction of ferrite $f_\alpha$ in the matrix, and the total carbon content of ductile iron $C_o$.

The model developed outlines the different stages of austenitization of the matrix of ductile iron in the presence of graphite nodules. The graphite nodules can act as the reservoir of carbon from where carbon diffuses out to the matrix austenite till an equilibrium is established between the austenite and graphite nodule at a given austenitization temperature.

## 3. Problem Formulation

In the present model, the time required for the austenitization of the matrix of ductile iron has been divided into two distinct stages. The first stage involves formation of austenite by dissolution of carbon from the matrix (if it contains pearlite) as well as from graphite nodule consuming all the preexisting phases in the matrix while the second stage for the homogenization of carbon in austenite takes place by dissolution of carbon from the graphite nodule located at the center of cell.

**Table 1 Symbols and units used in the model**

| Symbol | Variable | Units |
|---|---|---|
| $C_o$ | Total carbon in the ductile iron | wt.% |
| $TC_{cell}$ | Total amount of carbon in the cell | wt.% |
| $TC_{nodule}$ | Total amount of carbon in the graphite nodule | wt.% |
| $TC_{matrix}$ | Total amount of carbon in the matrix of the cell | wt.% |
| $TC_\gamma$ | Total carbon content in austenite layer of thickness $l_\gamma$ | wt.% |
| $TC(s)$ | Total amount of carbon in austenite cell as a function of diffusion distance $s$ | wt.% |
| $TC(b)$ | Total amount of carbon in austenite cell as a function of carbon content in austenite at the cell boundary | wt.% |
| $\rho_o$ | Density of ductile iron | gm/cm$^3$ |
| $\rho_m$ | Density of the matrix ductile iron | gm/cm$^3$ |
| $\rho_g$ | Density of graphite | gm/cm$^3$ |
| $\rho_\gamma$ | Density of austenite | gm/cm$^3$ |
| $r_{cell}$ | Radius of cell | mm |
| $r_g$ | Radius of graphite nodule | mm |
| $C_{\gamma g}$ | Carbon content in austenite at the graphite/austenite interface | wt.% |
| $C_{\alpha g}$ | Carbon content in ferrite at the graphite/ferrite interface | wt.% |
| $C_{\gamma\alpha}$ | Carbon content in austenite at the austenite/ferrite interface | wt.% |
| $l_\gamma$ | Thickness of austenite which dissolves carbon from the graphite nodule during austenitization | mm |
| $l_\gamma^m$ | Maximum possible value of $l_\gamma$ in a given ductile iron | mm |
| $J$ | Flux of carbon per unit time | atoms/cm$^2$/s |
| $D_C^\gamma$ | Diffusion coefficient of carbon in austenite | mm$^2$s$^{-1}$ |
| $f_\alpha$ | Volume fraction of ferrite in cast matrix | |

## 4. Mathematical Modeling

### 4.1 Formation of Austenite

Austenite may be presumed to develop surrounding the graphite nodule when a ductile iron with carbon content $C_o$ is austenitized at austenitization temperature $T_\gamma$. At this temperature, no equilibrium exists between ferrite and graphite. Austenite can exist in equilibrium with graphite as well as with ferrite at this temperature. Two dissolution processes will accompany the process of austenitization: (a) the dissolution of matrix carbide if the matrix contains pearlite and (b) the dissolution of carbon from the graphite nodule since overall matrix composition is lower than saturation carbon level $C_{\gamma g}$ of austenite, which is in equilibrium with graphite. Because the carbide lamellae in pearlite have larger surface area and are relatively thin, it may be presumed that the dissolution of matrix carbides may take place in relatively short time. The formation of austenite is controlled by dissolution of carbon from the graphite nodules involving diffusion over large distances. The analysis is carried out below for an individual cell.

The total amount of the carbon in a cell $TC_{cell}$ is:

$$TC_{cell} = \frac{4}{3}\pi r_{cell}^3 \rho_o C_o \quad \text{(Eq 1)}$$

where $\rho_o$ is the density of the ductile iron. The total carbon content of the cell is distributed in the graphite nodule and the matrix. The amount of carbon in graphite nodule $TC_{nodule}$ is given by:

$$TC_{nodule} = \frac{4}{3}\pi r_g^3 \rho_g \quad \text{(Eq 2)}$$

where $\rho_g$ is the density of graphite nodule of radius $r_g$. The amount of carbon in the matrix of the cell $TC_{matrix}$ may be obtained by subtracting $TC_{nodule}$ from $TC_{cell}$ as:

$$TC_{matrix} = \frac{4}{3}\pi r_{cell}^3 \left[ (\rho_o C_o) - \rho_g \left( \frac{r_g}{r_{cell}} \right)^3 \right] \quad \text{(Eq 3)}$$

When the equilibrium is attained between austenite and the graphite nodule at the end of austenitization at a temperature $T_\gamma$, the carbon content of austenite should be $C_{\gamma g}$. The additional amount of carbon that is required by the matrix to attain this state is:

$$TC_{ADD} = \frac{4}{3}\pi (r_{cell}^3 - r_g^3)\rho_m C_{\gamma g} - TC_{matrix} \quad \text{(Eq 4)}$$

where, $\rho_m$ is the density of the matrix and $C_{matrix}$ is the carbon content of the matrix. The shrinking size of graphite nodule due to dissolution has been neglected. This additional amount of carbon $TC_{ADD}$ is supplied to the matrix by dissolution of carbon from the graphite nodule located at the center of the cell, resulting in progressive thickening of the layer of austenite around the graphite nodule. If $l_\gamma$ is the thickness of the austenite layer at time $t$ and one assumes that a steady concentration profile may be established within the austenite layer, the following approximation can be made:

$$C_\gamma = C_{\gamma g} - \frac{(r_g + l_\gamma)}{r \times l_\gamma} \times (r - r_g) \times (C_{\gamma g} - C_{\gamma\alpha}) \text{ for } r_g \le r \le r_g + l_\gamma \quad \text{(Eq 5)}$$

where $C_\gamma$ is the carbon content in the austenite layer at a distance $r$ from the center of the cell. $C_{\gamma g}$ is the saturation carbon content of austenite, in equilibrium with graphite, and $C_{\gamma\alpha}$ is the carbon content of austenite, in equilibrium with ferrite in the matrix.

Figure 2 gives the schematic representation of the concentration profile in a cell at any time $t$ during this process. The total carbon content in the austenite-layer of thickness $l_\gamma$ and density $\rho_\gamma$ is $TC_\gamma$ and it is given by:

$$TC_\gamma = \rho_\gamma \int_{r_g}^{r_g + l_\gamma} 4\pi r^2 \, dr C_\gamma \quad \text{(Eq 6)}$$

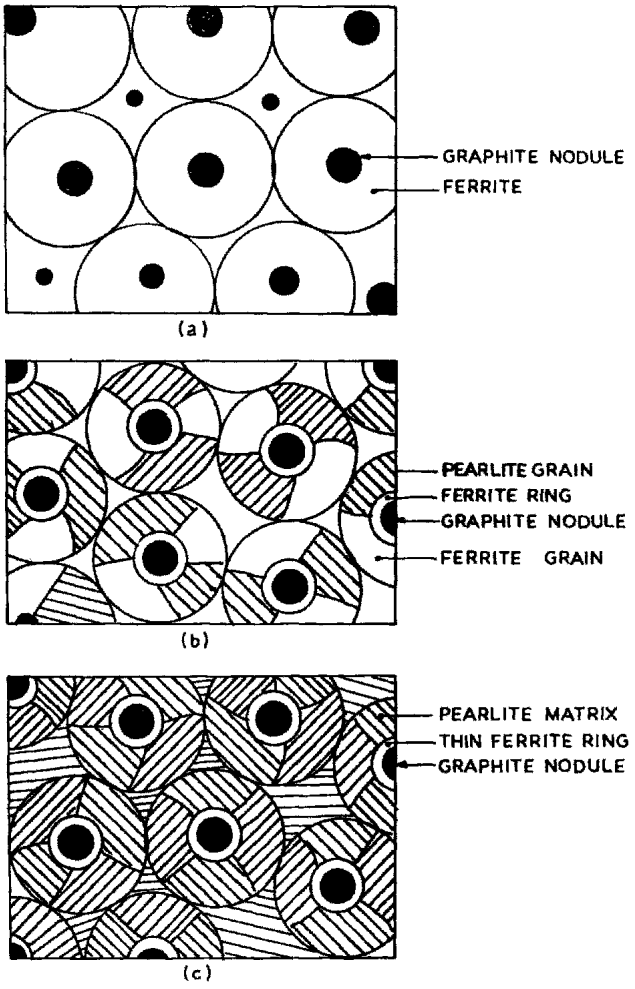


**Fig. 1** Schematic representation of different types of ductile irons

$$TC_\gamma = \frac{2\pi}{3}\rho_\gamma l_\gamma [C_{\gamma g} r_g (3r_g + l_\gamma) + C_{\gamma\alpha}(3r_g^2 + 5r_g l_\gamma + 2l_\gamma^2)] \quad \text{(Eq 7)}$$

For sustaining a growth of $dl_\gamma/dt$ of the austenite layer, the required rate of carbon accumulation in the layer is $dTC_\gamma/dt$ as given below:

$$\frac{dTC_\gamma}{dt} = \frac{2\pi}{3}\rho_\gamma [C_{\gamma g} r_g (3r_g + 2l_\gamma) + C_{\gamma\alpha}(3r_g^2 + 10 r_g l_\gamma + 6l_\gamma^2)]\frac{dl_\gamma}{dt} \quad \text{(Eq 8)}$$

It may be reasonably presumed that all the carbon that is able to diffuse through the γ-layer to γ/α interface is for the transformation of α to γ for the thickening of γ-layer.

Under steady state, the carbon diffusing through austenite is reaching γ/α interface, and the flux of carbon at γ/α interface at $r = r_g + l_\gamma$ is estimated following Fick's first law as:

$$J_1 = -D_{C^\gamma}\rho_\gamma 4\pi r^2 \frac{dC_\gamma}{dr} = 4\pi D_{C^\gamma}\rho_\gamma \frac{r_g}{l_\gamma}(r_g + l_\gamma)(C_{\gamma g} - C_{\gamma\alpha}) \quad \text{(Eq 9)}$$

As the thickness of the austenite layer around graphite nodule increases, the flux of solute comes down. It has already been argued that to sustain growth of austenite at the rate of $dl_\gamma/dt$, one has to have $dTC_\gamma/dt$, and so the rate of growth has

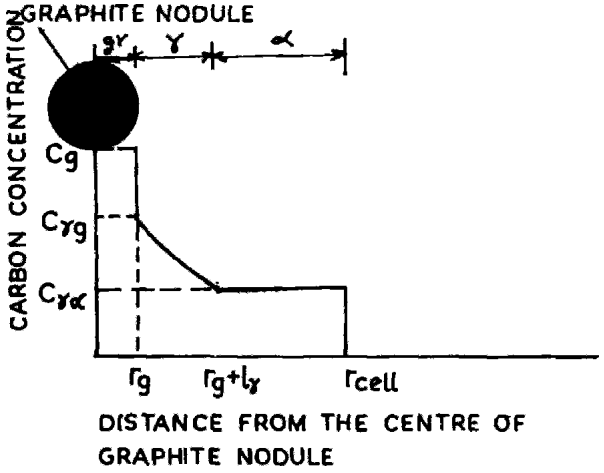


**Fig. 2** Schematic representation of carbon concentration profile at any time, *t,* when austenite layer has grown to a thickness, $l_\gamma$, surrounding graphite nodule

to reduce with increasing thickness of the austenite layer as to satisfy,

$$J_1 = \frac{dTC_\gamma}{dt} \quad \text{(Eq 10)}$$

Substituting from Eq 8 and 9 in Eq 10,

$$4\pi D_{C^\gamma}\rho_\gamma \frac{r_g}{l_\gamma}(r_g + l_\gamma)(C_{\gamma g} - C_{\gamma\alpha}) = \frac{2\pi}{3}\rho_\gamma [C_{\gamma g} r_g (3r_g + 2l_\gamma) + C_{\gamma\alpha}(3r_g^2 + 10 r_g l_\gamma + 6l_\gamma^2)]\frac{dl_\gamma}{dt} \quad \text{(Eq. 11)}$$

Rewriting the above equation and integrating one gets,

$$6D_{C^\gamma}\int_0^t dt = \frac{C_{\gamma g}}{(C_{\gamma g} - C_{\gamma\alpha})}\int_0^{l_\gamma}\left(3 - \frac{l_\gamma}{r_g + l_\gamma}\right) l_\gamma dl_\gamma + \frac{C_{\gamma\alpha}}{(C_{\gamma g} - C_{\gamma\alpha})}\int_0^{l_\gamma}\left[3l_\gamma + \frac{7l_\gamma}{r_g} - \frac{l_\gamma^3}{r_g(r_g + l_\gamma)}\right] dl_\gamma \quad \text{(Eq 12)}$$

since at $t = 0$, $l_\gamma = 0$. At any time $t$ the austenite layer grows to a thickness $l_\gamma$.

For short time $t$, when $l_\gamma \ll r_g$, one may ignore higher order terms in $l_\gamma$ and arrive at the following approximate equation:

$$6D_{C^\gamma}t = \frac{3}{2}\times\frac{(C_{\gamma g} + C_{\gamma a})}{(C_{\gamma g} - C_{\gamma a})} l_\gamma^2 \quad \text{(Eq 13)}$$

Thus, $l_\gamma$ may grow with time following parabolic $t^{1/2}$ behavior for a short period of austenitization.

When $l_\gamma \gg r_g$, one may rewrite Eq 12 as:

$$6D_{C^\gamma}\int_0^t dt = \frac{C_{\gamma g}}{(C_{\gamma g} - C_{\gamma\alpha})}\int_0^{l_\gamma}\left(2 - \frac{r_g}{l_\gamma} - \frac{r_g^2}{l_\gamma^2}\right) l_\gamma dl_\gamma$$

$$+\frac{C_{\gamma\alpha}}{(C_{\gamma g}-C_{\gamma\alpha})}\int_0^{l_\gamma}\left(4l_\gamma-7r_g+\frac{6l_\gamma^2}{r_g}\right)\mathrm{d}l_\gamma \qquad \text{(Eq 14)}$$

Retaining only up to $(r_g)^0$ terms,

$$6D_{C^\gamma}t=\frac{C_{\gamma g}}{(C_{\gamma g}-C_{\gamma\alpha})}l_\gamma^2+\frac{C_{\gamma\alpha}}{(C_{\gamma g}-C_{\gamma\alpha})}\times 2l_\gamma^2\left(\frac{l_\gamma}{r_g}+1\right) \qquad \text{(Eq 15)}$$

The maximum thickness, $l_\gamma^m$ possible in a given ductile iron may be related to the volume fraction of austenite formed by the dissolution of carbon from the graphite nodule. Let us consider a ductile iron, which contains $f_\alpha$ volume fraction of ferrite in the matrix excluding that in pearlite. It may be expected that the volume fraction of pearlite in the matrix of ductile iron i.e., $(1-f_\alpha)$ will transform to austenite relatively faster, where as the ferrite of the matrix may even transform till the time when carbon content of austenite reaches the limiting composition of $C_{\gamma\alpha}$.

Thus, the volume fraction of austenite formed through dissolution of carbide of pearlite in the matrix in austenite $f_\gamma^C$ may be related to the volume fraction of pearlite $(1-f_\alpha)$ of the matrix as:

$$f_\gamma^C=(1-f_\alpha)\times\frac{0.68}{C_{\gamma\alpha}} \qquad \text{(Eq 16)}$$

The remaining matrix volume in the cell may transform to austenite only by dissolution of carbon from the nodule, and it is given by $(1-f_\gamma^C)$. This volume fraction of austenite formed by the dissolution of carbon from the graphite nodule may be written in terms of the maximum thickness of the austenite region $l_\gamma^m$ formed around the graphite nodule. This gives:

$$(1-f_\gamma^C)(r_{cell}^3-r_g^3)=\{(r_g+l_\gamma^m)^3-r_g^3\} \qquad \text{(Eq 17)}$$

On simplification of Eq 17, the maximum thickness of the austenite layer forming around the graphite nodule by the dissolution of carbon from the graphite nodule of cell $l_\gamma^m$ may be written in terms of $r_g$, $r_{cell}$, and $f_\gamma^C$:

$$l_\gamma^m=[r_{cell}^3\times(1-f_\gamma^C)+f_\gamma^C\times r_g^3]^{1/3}-r_g \qquad \text{(Eq 18)}$$

The time $t_\gamma$ when the entire matrix of the ductile iron has transformed to austenite may be estimated approximately from Eq 15 by substituting $l_\gamma = l_\gamma^m$ as:

$$t_\gamma=\frac{C_{\gamma g}}{(C_{\gamma g}-C_{\gamma\alpha})}\frac{(l_\gamma^m)^2}{6D_{C^\gamma}}+\frac{C_{\gamma\alpha}}{(C_{\gamma g}-C_{\gamma\alpha})}\frac{(l_\gamma^m)^2}{3D_{C^\gamma}}\left(\frac{l_\gamma^m+r_g}{r_g}\right) \qquad \text{(Eq 19)}$$

At time $t_\gamma$, the austenite formed by the dissolution of carbon from nodule has grown to the maximum thickness of $l_\gamma^m$. The concentration profile in the austenite may be given schematically, as shown in Fig. 3.

### 4.2 Homogenization of Austenite

Once the austenite layer growing around graphite nodule reaches the maximum thickness of $l_\gamma^m$, there is further dissolution of carbon from the graphite nodule to enrich and homogenize austenite matrix in the cell. One may presume two distinct phases of homogenization of concentration of carbon in austenite, in a two-phase region of austenite and graphite by dissolution of carbon from the graphite nodule located at the center of the cell: (a) increasing the diffusion distance from $r_g$ to $r_{cell}$ and (b) increasing the level of carbon at $r_{cell}$, eventually reaching the saturation level when a homogeneous matrix of austenite is achieved in the two phase region of austenite and graphite.

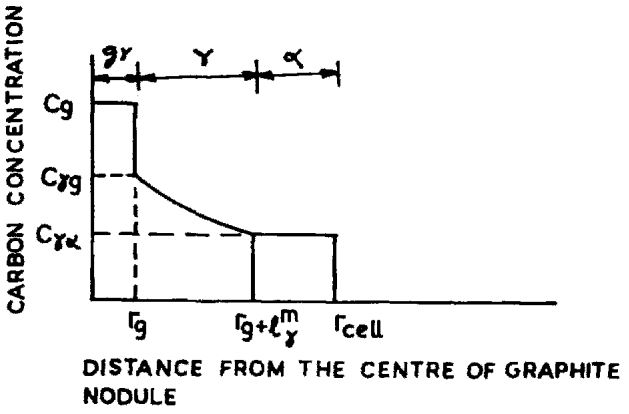


**Fig. 3** Schematic representation of carbon concentration profile at any time, $t_\gamma$, when austenite layer has grown to a thickness, $l_\gamma^m$, surrounding graphite nodule

**4.2.1 Homogenization of Austenite: Phase (a).** The schematic profile of carbon concentration at any time during phase (a) of homogenization of austenite is given in Fig. 4. The carbon concentration profile given in Eq 5 could be linearized and may be written as:

$$C_\gamma=C_{\gamma g}-\frac{(C_{\gamma g}-C_{\gamma\alpha})}{s}(r-r_g)\ \text{for}\ r_g\le r\le r_g+s \qquad \text{(Eq 20)}$$

where $C_\gamma$ is the carbon content in the austenite cell at a distance $r$ from the center of the nodule during phase (a) of homogenization of austenite, and $s$ is the diffusion distance at a given time. The concentration gradient is given as:

$$\frac{\mathrm{d}C}{\mathrm{d}r}=-\frac{C_{\gamma g}-C_{\gamma\alpha}}{s} \qquad \text{(Eq 21)}$$

where $\mathrm{d}C/\mathrm{d}r_s$ is the concentration gradient at any distance $r = r_g + s$ from the center of the nodule,

Total carbon in the austenite cell $TC(s)$, which is a function of diffusion distance $s$ is given by:

$$TC(s)=\frac{4}{3}\pi\rho_\gamma(r_{cell}^3-r_g^3)C_{\gamma\alpha}+4\pi\rho_\gamma\int_{r_g}^{r_g+s}(C_\gamma-C_{\gamma\alpha})r^2\mathrm{d}r \qquad \text{(Eq 22)}$$

where $l_\gamma^m \le s \le r_{cell} - r_g$.

Putting the value of $C_\gamma$ from Eq 20 in Eq 22, one gets:

$$TC(s)=\frac{4}{3}\pi\rho_\gamma(r_{cell}^3-r_g^3)C_{\gamma\alpha}+4\pi\rho_\gamma\int_{r_g}^{r_g+s}(C_{\gamma g}-C_{\gamma\alpha})\left[r^2-\frac{r-r_g}{s}r^2\right]\mathrm{d}r$$
$$=\frac{4}{3}\pi\rho_\gamma(r_{cell}^3-r_g^3)C_{\gamma\alpha}+\frac{\pi\rho_\gamma}{3}(C_{\gamma g}-C_{\gamma\alpha})(s^3+4r_gs^2+6r_g^2s) \qquad \text{(Eq 23)}$$

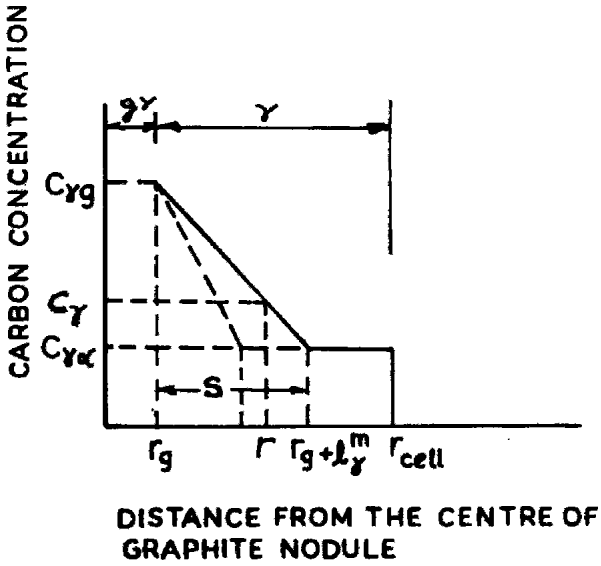


**Fig. 4** Schematic representation of concentration profile of carbon in austenite during phase (a) of the homogenization of austenite

Now the rate of increase of diffusion distance with time, d$s$/d$t$, determines the rate of accumulation of carbon in austenite, d$TC(s)$/d$t$, as given by Eq 23.

$$\frac{\mathrm{d}TC(s)}{\mathrm{d}s} = \frac{\pi\rho_\gamma}{3}(C_{\gamma g} - C_{\gamma\alpha})(3s^2 + 8r_g s + 6r_g^2) \quad \text{(Eq 24)}$$

The rate of change in total carbon with time, d$TC(s)$/d$t$ is equal to the flux of carbon entering austenite from graphite nodule at the center of the cell. The flux of carbon through austenite per unit time for the given concentration profile may be estimated following Fick's first law as:

$$J_2 = -D_{C\gamma}4\pi r^2\rho_\gamma\frac{\mathrm{d}C}{\mathrm{d}r} = D_{C\gamma}4\pi r^2\rho_\gamma\frac{C_{\gamma g} - C_{\gamma\alpha}}{s} \quad \text{(Eq 25)}$$

As the carbon diffuses through austenite, $s$ shifts to a longer distance in the austenite matrix, away from around the graphite nodule, thereby decreasing the slope of concentration profile around the graphite nodule and consequently, the flux of carbon. To sustain increasing diffusion distance at a rate of d$s$/d$t$, one has to have d$TC(C)$/d$t$, which should satisfy,

$$J_2 = \frac{\mathrm{d}TC(C)}{\mathrm{d}t} = \frac{\mathrm{d}TC(C)}{\mathrm{d}s}\times\frac{\mathrm{d}s}{\mathrm{d}t} \quad \text{(Eq 26)}$$

Substituting d$TC(s)$/d$s$ and $J_2$ from Eq 24 and 25, respectively, in Eq 26, one gets:

$$D_{C\gamma}4\pi r^2\rho_\gamma\frac{C_{\gamma g} - C_{\gamma\alpha}}{s} = \frac{\pi\rho_\gamma}{3}(C_{\gamma g} - C_{\gamma\alpha})(3s^2 + 8r_g s + 6r_g^2)\frac{\mathrm{d}s}{\mathrm{d}t}$$

$$= \frac{\pi\rho_\gamma}{3}(C_{\gamma g} - C_{\gamma\alpha})(3s^2 + 8r_g s + 6r_g^2)\frac{\Delta s}{\Delta t_1} \quad \text{(Eq 27)}$$

Therefore, the time required for carbon to diffuse into austenite from the graphite/austenite interface to result in a diffusion distance $s$ is given as:

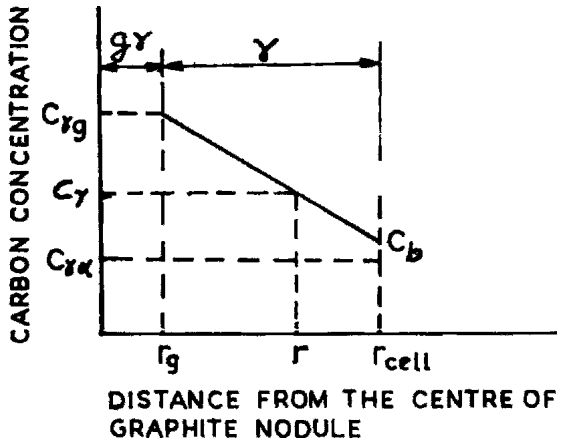


**Fig. 5** Schematic representation of concentration profile of carbon in austenite during phase (b) of homogenization of austenite

$$\Delta t_1 = \frac{3s^3 + 8r_g s^2 + 6r_g^2 s}{12D_C^\gamma r_g^2}\times\Delta s \quad \text{(Eq 28)}$$

where $\Delta s = r - r_g - l_\gamma^m$.

**4.2.2 Homogenization of Austenite: Phase (b).** This phase of homogenization of austenite starts after attaining $s = l_\gamma^m$ at the end of phase (a) of homogenization. The schematic profile of carbon concentration at any time $t$, during homogenization of austenite is given in Fig. 5. The carbon concentration profile for phase (b) in austenite may be written as:

$$C_\gamma = C_{\gamma g} - \frac{C_{\gamma g} - C_b}{r_{cell} - r_g}(r - r_g) \text{ for } r_g \le r \le r_{cell} \quad \text{(Eq 29)}$$

where $C_\gamma$ is the carbon content in the austenite cell at distance $r$ from the center of the nodule and $C_b$ is the concentration of carbon in austenite at the cell boundary. The concentration gradient may be given as:

$$\frac{\mathrm{d}C}{\mathrm{d}r} = -\frac{C_{\gamma g} - C_b}{r_{cell} - r_g} \quad \text{(Eq 30)}$$

The total amount of carbon $TC(C_b)$ in the austenite cell of radius $r_{cell}$ is a function of carbon concentration $C_b$ at the cell boundary and is estimated from Eq 29 as:

$$TC(C_b) = \frac{4}{3}\pi\rho_\gamma(r_{cell}^3 - r_g^3)C_b + 4\pi\rho_\gamma\int_{r_g}^{r_{cell}}(C_{\gamma g} - C_b)\left[1 - \frac{(r - r_g)}{(r_{cell} - r_g)}\times r^2 dr\right] \quad \text{(Eq 31)}$$

where $C_{\gamma\alpha} \le C_b \le C_{\gamma g}$. After integration, Eq 31 becomes:

$$TC(C_b) = \frac{4}{3}\pi\rho_\gamma(r_{cell}^3 - r_g^3)C_b + \frac{\pi\rho_\gamma}{3}\frac{(C_{\gamma g} - C_{\gamma\alpha})}{(r_{cell} - r_g)}[r_{cell}^4 - 4r_g^3 r_{cell} + 3r_g^4]$$

$$= \frac{4}{3}\pi\rho_\gamma(r_{cell}^3 - r_g^3)C_b + \frac{\pi\rho_\gamma}{3}(C_{\gamma g} - C_b)[r_{cell}^3 - 4r_{cell}^2 r_g + r_{cell}r_g^2 - 3r_g^3] \quad \text{(Eq 32)}$$

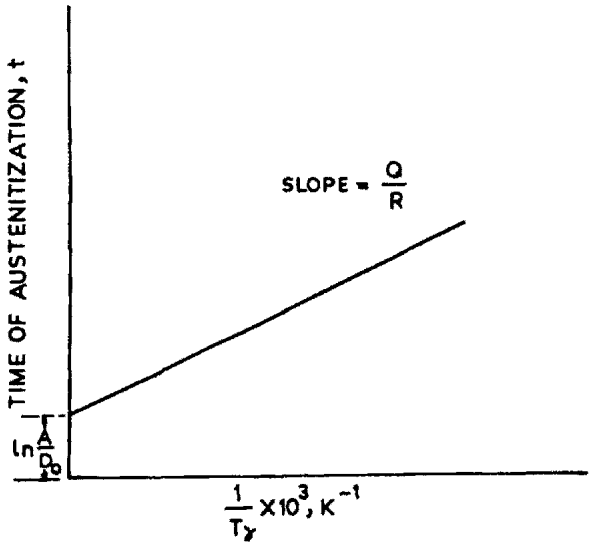


**Fig. 6** Variation of time of austenitization with austenitization temperature

For a carbon enrichment rate of $dC_b/dt$ at the cell boundary, the corresponding rate of accumulation of carbon in the austenite matrix is $dTC(C_b)/dt$ and it may be evaluated from Eq 32.

$$\frac{dTC(C_b)}{dC_b} = \frac{4}{3}\pi\rho_\gamma(r_{cell}^3 - r_g^3) - \frac{\pi\rho_\gamma}{3}[r_{cell}^3 + r_{cell}^2 r_g + r_{cell} r_g^2 - 3r_g^3]$$
$$= \frac{\pi}{3}\rho_\gamma(3r_{cell}^2 - r_{cell}^2 r_g - r_{cell} r_g^2 - r_g^3) \quad \text{(Eq 33)}$$

The flux of carbon $J_3$ from the graphite nodule to the austenite matrix per unit time for the given concentration profile in Eq 20 may be estimated using Fick's first law as:

$$J_3 = -D_C^\gamma 4\pi r^2 \rho_\gamma \frac{dC}{dr} = D_C^\gamma 4\pi r_g^2 \rho_\gamma \frac{C_{\gamma g} - C_b}{r_{cell} - r_g} \quad \text{(Eq 34)}$$

The rate of change of total carbon in austenite with time, $dTC(C)/dt$, is equal to the flux of carbon atoms entering austenite across graphite/austenite interface; therefore:

$$J_3 = \frac{dTC(C_b)}{dt} = \frac{dTC(C_b)}{dC} = \frac{dC}{dt} = \frac{dTC(C_b)}{dC} \times \frac{\Delta C}{\Delta t} \quad \text{(Eq 35)}$$

Substituting Eq 33 and 34 into 35, one gets:

$$D_C^\gamma 4\pi r_g^2 \rho_\gamma \frac{C_{\gamma g} - C_b}{r_{cell} - r_g} = \frac{\pi\rho_\gamma}{3}[3r_{cell}^3 - r_{cell}^2 r_g - r_{cell} r_g^2 - r_g^3]\frac{\Delta C}{\Delta t_2} \quad \text{(Eq 36)}$$

The time required for austenite to achieve a given carbon concentration of $C_b$ is given by:

$$\Delta t_2 = \frac{3r_{cell}^4 - 4r_{cell}^3 r_g + r_g^4}{12 D_C^\gamma r_g^2} \times \Delta C \text{ where } \Delta C$$
$$= C_b - C_{\gamma\alpha} \text{ for } C_b > C_{\gamma\alpha} \quad \text{(Eq 37)}$$

**Table 2 Composition of irons used in present work**

| Element | Composition, wt.% | | |
|---|---|---|---|
| | Iron I | Iron II | Iron III |
| C | 3.43 | 3.60 | 3.48 |
| Si | 3.02 | 2.20 | 2.028 |
| Mn | 0.287 | 0.40 | 0.22 |
| P | 0.016 | 0.02 | 0.05 |
| S | 0.007 | 0.003 | 0.004 |
| Cr | … | 0.017 | 0.05 |
| Mo | 0.43 | 0.06 | 0.33 |
| Cu | … | 0.40 | 0.60 |
| Ni | 1.160 | 0.07 | 0.016 |
| Ti | … | … | 0.04 |
| Mg | 0.12 | 0.04 | 0.04 |
| Sn | … | … | 0.0079 |
| V | … | … | 0.012 |
| Al | … | … | 0.02 |
| Fe | Remaining | Remaining | Remaining |

**Table 3 Microstructural characteristics of ductile irons**

| Characteristics | Iron I | Iron II | Iron III |
|---|---|---|---|
| Equivalent ASTM grade | 450/10 | 500/7 | 600/3 |
| Nodule count, $mm^{-2}$ | 100 | 150 | 250 |
| Amount of ferrite in the cast matrix, % | 99 | 20 | 5 |
| Amount of pearlite in the cast matrix, % | 1 | 80 | 95 |
| Average radius of graphite, $r_g$, mm | 0.02 | 0.014 | 0.01 |
| Average size of the cell, $r_{cell}$, mm | 0.07 | 0.04 | 0.03 |
| Initial Matrix hardness, Hv20 | 188 | 245 | 260 |

### 4.3 Total Time Required for Complete Austenitization

The total time $t$ required for complete austenitization process may be given as the sum of the time required for the transformation to austenite, $t_\gamma$ the time required for the homogenization of carbon content in austenite, which consists of two phases (a) the time required for the diffusion distance $s$ to move up to the boundary of the cell $\Delta t_1$ and (b) the time required for the carbon concentration at the cell boundary to attain $C_{\gamma g}$. Thus:

$$\text{Total time, } t = t_\gamma + \Delta t_1 \theta(s - l_\gamma^m) + \Delta t_2 \theta(C_b - C_{\gamma\alpha}) \quad \text{(Eq 38)}$$

where $\theta(x)$ is a step function and

$$\theta(x) = \begin{cases} 0, \text{ for } x < 0 \\ 1, \text{ for } x \geq 0 \end{cases}$$

The total time of austenitization $t$ given in Eq 38 may be written explicitly from Eq 19, 28, and 37 as:

$$t = A\frac{1}{D_C^\gamma} \quad \text{(Eq 39)}$$

where

$$A = \frac{C_{\gamma g} \times l_\gamma^{m^2}}{6(C_{\gamma g} - C_{\gamma\alpha})} + \frac{C_{\gamma\alpha} \times l_\gamma^{m^2} \times (l_\gamma^m + r_g)}{r_g(C_{\gamma g} - C_{\gamma\alpha})} + \frac{3s^3 + 8r_g s^2 + 6r_g^2 s}{12r_g^2} \times \Delta s$$
$$+ \frac{3r_{cell}^4 - 4r_{cell}^3 r_g + r_g^4}{12r_g^2} \times \Delta C \quad \text{(Eq 40)}$$

**Table 4 Variation of microhardness of the austenite (martensite on quenching) of ductile iron with distance from the graphite nodule surface in Iron I**

| Sample | Distance from graphite nodule, mm | Microhardness after different time periods VHN, 100 g | | | | |
|---|---|---|---|---|---|---|
| | | 2 min | 5 min | 15 min | 25 min | 35 min |
| 1 | 0.01 | 375 | 463 | 540 | 607 | 635 |
| 2 | 0.02 | 345 | 463 | 540 | 607 | 635 |
| 3 | 0.03 | 303 | 433 | 520 | 597 | 635 |
| 4 | 0.04 | 255 | 403 | 500 | 587 | 635 |

**Table 5 Comparison in the time for complete austenitization in three ductile irons of theoretical and experimental results**

| Iron | Equilibrium content, wt.% | Time of austenitization, min (as calculated from the model) | | | | Time of austenitization, min (Experimental) |
|---|---|---|---|---|---|---|
| | | $t_\gamma$ | $\Delta t_1$ | $\Delta t_2$ | $t$ | |
| Iron I | 0.75 | 1.5 | 11 | 17 | 29.5 | 35 |
| Iron II | 0.82 | 0.9 | 3.2 | 1.1 | 5.2 | 10 |
| Iron III | 0.85 | 0.05 | 2.6 | 0.53 | 3.2 | 2 |

Since $D_C^\gamma = D_o \exp^{-Q/RT}$, the time $t$ may be rewritten as:

$$t = \frac{A}{D_o} e^{+Q/RT} \quad \text{(Eq 41)}$$

Taking log on both sides, one may write:

$$\ln(t) = \ln \frac{A}{D_o} + \frac{Q}{RT_\gamma} \quad \text{(Eq 42)}$$

The logarithm of the time of austenitization $t$ is plotted as a function of reciprocal of austenitization temperature $T_\gamma$. The straight-line relationship between the time and temperature of austenitization, with slope of $+Q/R$ and the intercept of the logarithm of $A/D_o$ on the $y$-axis, from Eq 42 is evident and is shown in Fig. 6.

## 5. Calculations of Austenitization Time Period

Using the above model, one could estimate the time required to achieve equilibrium carbon content in austenite on austenitization of a particular ductile iron at a given temperature. The predictions of this model were tested on three ductile irons prepared in a commercial foundry using an induction-melting furnace and cast in the shape of one in Y blocks. Their compositions are given in Table 2. The microstructural characteristics of these irons are given in Table 3. The specimens ($55 \times 10 \times 10$) mm$^3$ machined from the leg part of Y block castings have been austenitized in a salt bath at 900 °C for different time periods of 2-120 min before quenching in water. To follow the austenitization kinetics, the change in carbon content of the matrix austenite (martensite on quenching) has been determined by the x-ray diffraction method using Cu $K_\alpha$ radiation on powder samples of water quenched specimens (Ref 7). The average carbon content of austenite in a two-phase region of austenite and graphite (transformed to martensite and graphite on quenching) reaches an equilibrium value of 0.75%, 0.82%, and 0.85% after 35, 10, and 2 min of austenitization at 900 °C for iron I, II, and III, respectively. The microhardness tests were performed on the matrix of quenched samples between two nodules from the nodule surfaces in order to verify the completion of austenitization using Vicker's hardness tester using a load of 100 g. The microhardness study ensures the microhardness value of the matrix between the two nodules is maximum and uniform corresponding to 35, 10, and 2 min of austenitization for irons I, II, and III, respectively, before which the microhardness is not uniform between the two nodules. Thus, these time periods may be taken as the times of completion of austenitization for the three ductile irons. Table 4 gives the variation of microhardness of austenite (martensite on quenching) of ductile iron with distance from the graphite nodule surface in Iron I. At a short time of austenitization, the hardness of austenite is higher near the nodule surface than that away from the nodule surface. However, after 35 min, the hardness becomes constant and uniform along the distance from the graphite nodule surface and thus provides an indirect indication of the evolution of concentration profile.

The mathematical model suggests that uniform carbon distribution in austenite with the equilibrium carbon content should be achieved in irons I, II, and III after 29.5, 5.2, and 3.24 min, respectively. Table 5 compares the theoretical as well as experimental austenitization time periods for austenitization of the three ductile irons with different initial microstructural characteristics. A reasonable agreement between estimated times for austenitization with the experimental results may be observed. Thus, the assumptions made for the simplification of the mathematical model are fairly reliable. It may be observed that the ductile iron with a higher volume fraction of ferrite in the cast structure requires a longer time for austenitization due to higher $l_\gamma$ and consequently longer $t_\gamma$ despite the lower equilibrium carbon content in the austenite $C_{\gamma g}$.

## 6. Conclusions

A mathematical model was developed to estimate the time required for austenitization of ductile iron leading to graphite nodules embedded in austenite of carbon content in

equilibrium with graphite. A number of assumptions have been made in the present work. The ductile iron is assumed to consist of spherical graphite nodules of uniform size. The matrix has been divided into spherical cells of the same size and austenitization has been studied in a cell. The austenitization time required to produce homogeneous austenite with equilibrium carbon content has been related to the structural parameters like radius of graphite nodule, radius of austenite cell, volume fraction of graphite, volume fraction of ferrite in cast matrix, and diffusion constant. The modeling methodology described in the present work provides a powerful tool to find the austenitization time required for complete austenitization in the two-phase region of austenite and graphite in ductile irons. Such an estimate of austenitization time helps to restrict the holding time so there is no significant grain growth in the resulting austenite. The estimated times for austenitization using the present model are in good agreement with those obtained through experimental work.

## References


1. T.N. Rouns, D.J. Moore, and K.B. Rundman, On the Structure and Mechanical Properties of Austempered Ductile Iron, *Trans. AFS,* Vol 92, 1984, p 815-840
2. A.S. Hamid Ali, K.I. Uzlov, N. Darwish, and R. Elliot, Austempering of Low Manganese Ductile Irons, Part 4: Relationship Between Mechanical Properties and Microstructure, *Mater. Sci. Technol.,* Vol 10, 1994, p 35-40
3. R. Warda, *Ductile Iron Data for Design Engineers,* QIT-Fer et Titane Inc., Montreal, Canada, 1990
4. R. Harding, Prospects for the Exploitation of ADI, *2nd International Conference on Austempered Ductile Iron,* ASME Gear Research Institute, Ann Arbor, MI, 1986, p 39-54
5. M. Grech and J.M. Young, Influence of Austempering Temperature on the Characteristics of Austempered Ductile Iron Alloyed with Cu and Ni, *AFS Trans.,* Vol 98, 1990, p 345
6. K. Ogi, A. Sawamoto, Y.C. Jin, and C.R. Loper, A Study of Some Aspects of Austenitization Process of Spheroidal Graphite Cast Iron, *AFS Trans.,* Vol 2, 1988, p 75-82
7. B.D. Cullity, *Elements of X-Ray Diffraction,* Addison Wesley Publishing Company, Inc., 1956, p 390-396